Subthalamic-pallidal interactions are critical in determining normal and abnormal functioning of the basal ganglia

Andrew Gillies, David Willshaw and Zhaoping Li [†]

Institute for Adaptive & Neural Computation, 5 Forrest Hill, University of Edinburgh, Edinburgh EH1 2QL, UK.
[†] Department of Psychology, University College, London, UK.

Correspondence to:

Andrew Gillies
Institute for Adaptive & Neural Computation
5 Forrest Hill
The University of Edinburgh
Edinburgh EH1 2QL
Scotland, UK

tel: +44 (0) 131 650 3096
fax: +44 (0) 131 650 4406
email: A.Gillies@anc.ed.ac.uk

Short title: **Subthalamic-pallidal interactions**

Subthalamic-pallidal interactions are critical in determining normal and abnormal functioning of the basal ganglia

Andrew Gillies, David Willshaw and Zhaoping Li [†]

Institute for Adaptive & Neural Computation, 5 Forrest Hill, University of Edinburgh, Edinburgh EH1 2QL, UK.
† Department of Psychology, University College, London, UK.

The subthalamic nucleus (STN) and external globus pallidus (GP) form a recurrent excitatory–inhibitory interaction within the basal ganglia. Through a computational model of these interactions we show that, under the influence of appropriate external input, the two nuclei can be switched between states of high and low activity or can generate oscillations consisting of bursts of high frequency activity repeated at a low rate. It is further demonstrated from the model that the generation of the repetitive bursting behaviour is favoured by increased inhibition of GP which is a condition indicated in Parkinson's disease. Paradoxically, increased striatal inhibition of GP is predicted to cause an increase rather than a decrease in its mean firing rate. These behaviours, arising from a biologically inspired computational model of the STN–GP interaction, have important consequences for basal ganglia function and dysfunction.

Keywords: basal ganglia, subthalamic nucleus, globus pallidus, bifurcation analysis, oscillatory behaviour.

1. INTRODUCTION

The basal ganglia (Fig. 1a) have been implicated in movement control and motor planning (Houk & Wise, 1995), motor and cognitive sequence generation (Suri & Schultz, 1998), sequence encoding (Beiser & Houk, 1998), context detection via reinforcement learning (Houk & Wise, 1995; Dominey *et al.*, 1995) and action selection (Redgrave *et al.*, 1999). There is growing realisation that processing within the basal ganglia is more complex than is implied in the classic view of a direct and an indirect pathway involving neocortex, basal ganglia and thalamus (Smith *et al.*, 1998; Alexander *et al.*, 1990). In particular, contemporary neuroanatomy of the basal ganglia reveals a prominent feedback system, involving the excitatory subthalamic nucleus and the inhibitory globus pallidus (Smith *et al.*, 1994; Joel & Weiner, 1997; Shink *et al.*, 1996; Wichmann & DeLong, 1999). STN projection neurons use glutamate as their primary neurotransmitter and exert a powerful excitatory influence on their targets (Kita, 1992). GP projection neurons use GABA (γ-Aminobutyric acid) as their primary neurotransmitter and exert an inhibitory influence on their targets (Smith & Bolam, 1989). STN is also subject to excitatory influences from cortex and from thalamus, whilst GP also receives inhibition from striatum (see Fig. 1a). In addition, local collaterals, suggesting significant interconnectivity within each nucleus, have been described (Kita *et al.*, 1983a; Iwahori, 1978; Kita & Kitai, 1994).

Recent analysis (Gillies & Willshaw, 1998) has suggested that the presence of even weak interconnectivity will cause the subthalamic nucleus to exhibit bistable behaviour. This means that the entire system can reside in a state in which all neurons fire at close to maximum rate, close to $500\,\mathrm{Hz}$, or in a state with a much lower firing rate. Short term excitatory input can shift the system into the high state and it was suggested that GP could provide inhibition to return it to the low state. This implies that large regions of the

3

STN can become uniformly and synchronously active as observed, for example, in rat STN after localised cortical stimulation (Fujimoto & Kita, 1993).

In culture preparations of the basal ganglia, Plenz & Kitai (1999) have recently reported electrical oscillations. The generation of the oscillations depends on the interaction between the GP and the STN which mirrors that observed in anatomical studies (Plenz *et al.*, 1998; Joel & Weiner, 1997). Rhythmic bursting oscillations have also been observed in STN neurons of MPTP monkeys (Nini *et al.*, 1995) and in human patients with Parkinson's disease (Levy *et al.*, 2000; Magariños-Ascone *et al.*, 2000). Some of the STN cells in these patients have a frequency matching that observed in tremor (5–6 Hz) and are influenced by tremor changes (Magariños-Ascone *et al.*, 2000). Other STN cells oscillate at higher frequencies ($\sim$15 Hz) with evidence of phase locking across the nucleus.

Understanding the underlying dynamics between STN and GP is essential to understanding these behaviours and how they may be modified or controlled. We have analysed the simplest representative circuit made up of an ensemble of excitatory STN neurons and an ensemble of inhibitory GP neurons (Fig. 1b). The dynamic behaviours observed in this simple system are essentially similar to those in larger scale systems. In the model, the STN neurons excite GP and are subject to excitation through local feedback and from cortex. Conversely, the GP neurons inhibit STN and are subject to inhibition through local feedback and from striatum. Analysis of this model has enabled us to identify the types of behaviour that this coupled STN–GP dynamical system can generate; in particular the conditions under which the system generates repetitive bursting.

2. METHODS

The STN–GP interaction is computed from coupled differential equations describing the mean membrane potentials x, y of populations of STN and GP neurons respectively:

$$\tau^{\text{STN}} \, dx/dt = -x + a\sigma(x) - c\xi(y) + I^{\text{CTX}}$$

$$\tau^{\text{GPe}} \, dy/dt = -y - b\xi(y) + d\sigma(x) + I^{\text{STR}}$$

(1)

τ^{STN} and τ^{GPe} are the time constants of the STN and GP neurons respectively. I^{CTX} and I^{STR} are external inputs from the cortex and striatum respectively. a, b, c and d specify connection strengths as indicated in Fig. 1b. $\sigma(x)$, and $\xi(y)$ are sigmoidal functions relating the STN and GP potentials x, y to their respective firing frequencies.

We present a mathematical analysis of this system along with accompanying simulation results to demonstrate the behaviours identified. For a general analysis of an excitatory–inhibitory oscillator system see Ermentrout & Cowan (1979). In our modified system, the equations are formulated in terms of membrane potential to allow direct application of experimental data (for example, derived voltage firing-rate curves, where the parameters specifying the shapes of the curves are derived from experimental data, see Table 1).

Our system is analysed and discussed within the context of STN/GP interactions and parameters. As the strengths of the external inputs and connections between and within STN and GP are substantially unconstrained, we explore how different strengths of neural connections can influence the types of behaviour the system may exhibit under different strengths of external inputs from cortex and from striatum. The external inputs are assumed to be constant for the period of analysis and we assume connection delays are negligible. We focus on the general physiological properties that reveal the most salient system behaviours. The model description and assumptions are at the level of general cell properties and the influence of individual channel types cannot be analysed within this

5

system. The behaviour of the model is characterised in terms of the potentials (x_0, y_0) at the equilibrium point, where $dx/dt = dy/dt = 0$, and the dynamic deviations from it. For more mathematical details see Box 1.

BOX 1 – MATHEMATICAL DETAILS

1. Formalisation. The coupled differential equations describing the membrane potentials x, y of the STN and GP neurons specify the ensemble average of a spike train model where impulses are convolved with an alpha type response function (see Shamma, 1989). This allows us to model spike trains in a dynamic manner:

$$\tau^{\text{STN}} \, dx/dt = -x + a\sigma(x) - c\xi(y) + I^{\text{CTX}}$$
$$\tau^{\text{GPe}} \, dy/dt = -y - b\xi(y) + d\sigma(x) + I^{\text{STR}} \tag{1}$$

where a, b, c, d specify the couplings within and between STN and GP; I^{CTX}, I^{STR} represent cortical and striatal influences. The STN and GP potentials x, y are related to firing frequency $\sigma(x), \xi(y)$ via sigmoidal functions:

$$\sigma(x) = \frac{\sigma_{\text{max}}}{1 + e^{-\kappa(x - x_{\text{th}})}} \qquad \xi(y) = \frac{\xi_{\text{max}}}{1 + e^{-\eta(y - y_{\text{th}})}} \tag{2}$$

2. Equilibrium points. The equilibrium values of (x, y) in Equation 1 are found by setting $dx/dt = dy/dt = 0$. The nature of these equilibria can be obtained by looking at the linear deviations $(\hat{x}, \hat{y})$ of (x, y) from the equilibrium point (x_0, y_0) as expressed by the matrix equation

$$\begin{pmatrix} d\hat{x}/dt \\ d\hat{y}/dt \end{pmatrix} = \mathbf{M} \begin{pmatrix} \hat{x} \\ \hat{y} \end{pmatrix}, \quad \text{where} \quad \mathbf{M} = \begin{pmatrix} -A & -C \\ D & -B \end{pmatrix},$$

$$\begin{aligned} A &\equiv \left(1 - a\sigma'(x_0)\right)/\tau^{\text{STN}} \\ B &\equiv \left(1 + b\xi'(y_0)\right)/\tau^{\text{GPe}} \\ C &\equiv c\xi'(y_0)/\tau^{\text{STN}} \\ D &\equiv d\sigma'(x_0)/\tau^{\text{GPe}} \end{aligned}$$

where $\sigma'(x_0)$ and $\xi'(y_0)$ are the derivatives of σ and ξ at (x_0, y_0). The deviations follow the solution $\hat{x} \propto e^{\lambda_{1,2} t}$ where $\lambda_{1,2}$ are the eigenvalues of $\mathbf{M}$

$$\lambda_{1,2} = -\frac{1}{2}(A + B) \pm \frac{1}{2}\sqrt{(A + B)^2 - 4(AB + CD)} \tag{3}$$

3. Nature of the equilibrium points. It is useful to distinguish the following three cases, which differ with respect to the signs of $A + B$ and $AB + CD$. Note that B, C, D are restricted to positive or zero values, whereas A, which depends on a, the amount of interconnectivity within STN, can have both positive and negative values.

3.1. $A + B > 0$ **and** $AB + CD > 0$. The eigenvalues $\lambda_{1,2}$ are real or complex with negative real parts, giving a stable equilibrium point.

3.2. $A + B < 0$ **and** $AB + CD > 0$. Both eigenvalues have positive real parts, giving an unstable equilibrium point. When the system has a single equilibrium point which is of this type, limit cycles (oscillations) result, as specified by the Poincaré-Bendixson theorem (Edelstein-Keshet, 1988).

3.3. $AB + CD < 0$. Both eigenvalues are real but with opposite signs, yielding an unstable saddle point from which deviations will reach one of the two separate basins.

4. Effect of changes in external inputs. Changing the cortical and striatal inputs by $\delta I^{\text{CTX}}, \delta I^{\text{STR}}$ change the equilibrium potentials (x_0, y_0) by

$$\delta x_o = \frac{B(\delta I^{\text{CTX}}/\tau^{\text{STN}}) - C(\delta I^{\text{STR}}/\tau^{\text{GPe}})}{AB + CD} \tag{4}$$

$$\delta y_o = \frac{D(\delta I^{\text{CTX}}/\tau^{\text{STN}}) + A(\delta I^{\text{STR}}/\tau^{\text{GPe}})}{AB + CD} \tag{5}$$

3. RESULTS

Setting of parameter values The parameters $\sigma_{\max}$, κ, x_{th} in $\sigma(x)$, $\xi_{\max}$, η, y_{th} in $\xi(y)$, τ^{STN} and τ^{GPe} are assigned values obtained from the experimental literature as given in Table 1.

Sources	Name	Value
STN		
Kita *et al.* (1983b); Afsharpour (1985),	τ^{STN}	$6\,\text{mS}$
	$\sigma_{\max}$	$500\,\text{Hz}$
Nakanishi *et al.* (1987).	x_{th}	$15\,\text{mV}$
	κ	$0.3\,\text{mV}^{-1}$
GP		
Kita & Kitai (1991),	τ^{GPe}	$14\,\text{mS}$
Nambu & Llinás (1994).	$\xi_{\max}$	$100\,\text{Hz}$
	y_{th}	$10\,\text{mV}$
	η	$0.2\,\text{mV}^{-1}$

Table 1: Parameter values used in the model.

We now describe the effects of varying the parameter values that remain unspecified, namely $a, b, c, d, I^{\text{CTX}}, I^{\text{STR}}$. We summarise the mathematical and numerical results which shed light on the following issues: (i) the function of the interconnectivity within STN; (ii) the effects of cortical and striatal input; (iii) the conditions under which the system is bistable; (iv) the conditions under which oscillations occur; (v) what determines the frequency of oscillations. An important factor is the value of a which determines the interconnectivity within STN.

The system can exist in three different types of state: single stable, bistable and oscillatory states. We first give an informal explanation of these states. STN and GP are subject to excitatory and inhibitory influences, mediated by external inputs and the connectivity parameters a, b, c, d. We consider the effects of gradually increasing the value of a, determining the amount of interconnectivity within STN. When a is small, giving little or no

self-excitation of STN, inhibition predominates, keeping the firing rates of both nuclei low and stable; there is a single stable state. For a higher value of a, the stable states of the system reflect the balancing out of the excitatory and inhibitory influences on the two nuclei. Stable states emerge at both high and low firing rates. For example, when the system is at rest with low firing rates, short term excitation of the STN from the cortex will increase the activity of the STN, pushing the entire system into a stable state with sustained high firing rates. Conversely, increased excitation of the GP whilst in this high state will increase the inhibition of itself and STN, ultimately driving both back to their low states (Fig. 2a). Both the high and low activity states are stable, and separating them is a barrier which can be crossed by external drive. This bistability causes the system to act in a "switch-like" manner. The oscillatory state could be regarded as alternating jumps, around the barrier, and between the high and low firing states which are not self-sustaining. The low frequency bursting–like oscillations emerge in both nuclei. Finally, for very large a and/or inputs I^{CTX}, excitation from STN predominates to keep both nuclei firing at a high rate.

We now give a more mathematically based description of the system states and their properties.

(i) *Interconnectivity within STN* If there is no interconnectivity, the STN-GP complex simply responds to its external input, by summing the afferent influences (from cortex and striatum); without interconnectivity it simply follows its transient input. The system resides at equilibrium and when disturbed will always return to this equilibrium. In this case $a = 0$ leading to $A > 0$ ($A \equiv (1 - a\sigma'(x_0))/\tau^{\text{STN}}$). This is condition **3.1** described in Box 1, where the state (x_0, y_0) is stable (see phase plot Fig. 3a).

(ii) *Influences of cortical and striatal input* In the presence of low levels of interconnectivity within the STN (small a) cortical excitation ***or*** *striatal inhibition* can lead to an *increase*

in the equilibrium firing rates of the STN and GP. Paradoxically, increased inhibition of GP can lead to an increase rather than a decrease in its mean firing rate (Fig. 2b). In particular, if a is sufficiently small that A is negative *yet $A + B$ and $AB + CD$ both remain positive*, all equilibrium points are stable (see case **3.1** and equations (4), (5)).

(iii) *Conditions under which bistable behaviour occurs*.

In previous work (Gillies & Willshaw, 1998) it was shown in a detailed model of the STN that it can display bistable behaviour. It can maintain activity at a high firing rate or at a low firing rate and can be driven between the two states by transient external input. A similar situation can occur in this coupled system. If a is sufficiently large so that A is sufficiently negative to make $AB + CD$ negative (case **3.3** of Box 1), the state (x_0, y_0) becomes an unstable saddle point. Two new stable states then appear, which will attract any deviation from (x_0, y_0) (see phase plot Fig. 3b, Fig. 2a), one at a high firing rate, the other at a low firing rate.

(iv) *Conditions for the generation of oscillations*. With the system in the bistable state, a sufficient increase in the value of a causes two (one stable and one unstable) of the three equilibrium points to disappear, the remaining equilibrium point becoming unstable (case **3.2**, Box 1). As the values of (x, y) are bounded, a limit cycle around this unstable point results, giving rise to oscillations in the values of x and y (Fig. 2c, Fig. 3c). The mathematics relating to this condition are summarised in Box 2. An important result is the relationship between external inputs and the onset of oscillations. As striatal inhibition is increased, *less* cortical input is needed for the system to enter the oscillatory state (Fig. 4).

(v) *Frequency of oscillations*. The frequency is proportional to $\sqrt{CD - (A - B)^2/4}$. This suggests that an increased x_0 (e.g. by increased cortical input) is likely to lead to lower oscillation frequencies due to a more negative $A < 0$. This is consistent with the converse

1. Existence of oscillations. Box 1 shows that oscillation occurs around a particular type of unstable fixed point which has $A + B < 0$ and $AB + CD > 0$. This unstable fixed point can arise out of a stable fixed point only by decreasing A to a negative value (since $B, C, D > 0$). This can be achieved by increasing interconnection a within STN and/or increasing $\sigma'(x_o)$ by shifting x_o via external drives I^{CTX} and I^{STR}. In the case in Fig. 2c, the parent (stable) fixed point is the one in Fig. 2b, and is the only fixed point of the system (Fig. 3a). In other cases, the parent fixed point can be one of the two stable fixed points among the 3 fixed points in the bistable condition (Fig. 3b). For instance, in our simulations, increasing a causes the unstable equilibrium point to coalesce with the lower stable fixed point. Increasing a further causes both to disappear, leaving just one equilibrium. This happens at the point at which the two curves $dx/dt = 0, dy/dt = 0$ drawn in the (x, y) plane have identical gradients near the fixed points. In both these cases, the single remaining equilibrium point (with $AB + CD > 0$) is unstable, taking complex eigenvalues with positive real values (case **3.2**, Box 1). According to the Poincaré-Bendixson theorem (Edelstein-Keshet, 1988), this implies the existence of limit cycles if both x and y are bounded. This is true in this case as both (x, y) are bounded from above and below. For example, from Equation (1), x is bounded as the sigmoidal functions are bounded $0 < \sigma(x) < \sigma_{max}$.

2. The onset of oscillations As a is increased, which causes a decrease in A, the value of $A + B$ for the stable fixed point moves from positive to zero, at which point oscillations occur:

$$A + B = (1 - a\sigma'(x_o))/\tau^{STN} + (1 + b\xi'(y_0))/\tau^{GPe} = 0 \qquad (6)$$

Under STN and GP resting conditions (rest firing rates $\sim$ 15Hz and $\sim$ 32Hz respectively(Féger *et al.*, 1991; Kita & Kitai, 1991)), x_0 is at the base of its sigmoid function $\sigma(x_0)$ giving a small value of $\sigma'(x_0)$. Increasing (x_0, y_0) by stronger cortical input I^{CTX} or striatal inhibition $(-I^{STR})$ leads to increased $\sigma'(x_0)$ eventually to give $A + B = 0$ (Equation (6)). This is demonstrated in the bifurcation diagram of Fig. 4. Either increased cortical input to STN or increased striatal input to GP can help bring about oscillations.

3. Frequency of oscillations. The frequency of the oscillations is approximated by the imaginary part of the eigenvalues $\lambda_{1,2}$. It is proportional to $\sqrt{CD - (A - B)^2/4}$

observation that cutting the cortical input to STN results in higher oscillation frequencies (Plenz & Kitai, 1999).

4. DISCUSSION

In our model of the STN–GP interaction, three types of behaviour have been identified: a single stable state (which is the only possible state in the absence of interactions within STN), a state in which the system acts as a bistable switch, being driven between the high and the low states by brief cortical or striatal stimulation; a state comprising synchronised, low frequency bursts of activity.

Assuming that the system has other functions than merely returning to a single stable state when disturbed from it, the bistable state could be interpreted as the normal mode of behaviour of the STN–GP system by means of which signals are provided from STN to the two output nuclei of the basal ganglia to provide control signals such as those for terminating movement (Gillies & Willshaw, 1998). The other mode of behaviour comprises synchronised, low frequency bursts of activity. These could be identified with such movement disorders as Parkinsonism and could be interpreted either as one of the normally occurring pacemaker activities that are unmasked by Parkinsonian conditions (Plenz & Kitai, 1999) or as an abnormally functioning state of the system.

Our model of the interactions between GP and STN can be used to characterise the oscillations generated by such a system under these abnormal conditions and to isolate what parameters are important in their generation, as follows:

(1) Assuming interactions within the STN, increased inhibition of GP from striatum is predicted to lead to an *increase* in firing rate in GP. This arises from the dynamic interaction between the STN and GP. Increased inhibition of the GP reduces its influence over the STN, allowing the interactions within the STN to increase STN activity resulting in increased ac-

tivity in the GP (Fig. 2b). Increased cortical excitation of STN also increases both STN and GP firing rate (Fig. 2d); see Results: (ii).

(2) The amount of excitatory cortical input to STN required to generate oscillations depends on the amount of striatal input to GP. As inhibitory striatal input to the GP is increased, the amount of excitatory drive required to generate oscillatory activity decreases (Fig. 4, Fig. 2c; see Results: (iv)). This prediction has important consequences for interpreting disorders of the basal ganglia. Under a current conceptual model of Parkinson's disease, striatal input to the GP is enhanced (Albin *et al.*, 1989). Our analysis demonstrates how this can lead to increased oscillatory activity in the STN–GP complex. In animal models of Parkinson's disease significantly increased oscillatory activity is observed in the STN and GP (Nini *et al.*, 1995; Bergman *et al.*, 1994). In human patients there is a significant population of rhythmic STN cells (Levy *et al.*, 2000; Magariños-Ascone *et al.*, 2000). This is a small population in comparison to observed phasic or tonic STN cell firing patterns (Magariños-Ascone *et al.*, 2000). Our model demonstrates the circuits that may underlie the generation of the rhythmic patterns while not ruling out other circuits and inputs that will allow cells to deviate from this rhythmic activity (e.g. via direct cortical input to the STN).

(3) The frequency of repetition of the high frequency bursts can vary in the model and it depends upon the strengths of connections between structures, time constants of the neurons and the external inputs (see Results: (v)). The range of oscillation frequencies observed within biologically realistic parameter regions in computer simulation is 3–25Hz. This fits well with burst frequencies found in *in vivo* monkey recordings under Parkinsonism type conditions (Nini *et al.*, 1995) and in recordings from human patients (Levy *et al.*, 2000; Magariños-Ascone *et al.*, 2000). This differs from cell culture studies (Plenz & Kitai, 1999) where the strength and extent of connections and external inputs are likely to differ

significantly from those found in *in vivo* recordings.

REFERENCES

Afsharpour, S. 1985 Light microscopic analysis of golgi–impregnated rat subthalamic neurons. *J. Comp. Neurol.*, **236**, 1–13.

Albin, R., Young, A., & Penny, J. 1989 Functional anatomy of basal ganglia disorders. *Trends in Neurosci.*, **12**, 366–375.

Alexander, G., Crutcher, M., & DeLong, M. 1990 Basal ganglia–thalamocortical circuits: Parallel substrates for motor, oculomotor, prefrontal, and limbic functions. In H. Uylings, C. Van Eden, J. De Bruin, M. Corner, & M. Freenstra, editors, *Progress in Brain Res.*, volume 85, pages 119–146. Elsevier Science, Oxford.

Beiser, D. & Houk, J. 1998 Model of cortical-basal ganglia ganglionic processing: encoding the serial order of sensory events. *J. Neurophysiology*, **79**, 3168–3188.

Bergman, H., Wichmann, T., Karmon, B., & DeLong, M. 1994 The primate subthalamic nucleus. ii. neuronal activity in the MPTP model of Parkinsonism. *J. Neurophysiology*, **72**, 507–520.

Dominey, P., Arbib, M., & Joseph, J. 1995 A model of corticostriatal plasticity for learning oculomotor associations and sequences. *J. Cognitive Neuroscience*, **7**, 311–336.

Edelstein-Keshet, L. 1988 *Mathematical Models in Biology*. McGraw–Hill Inc., New York.

Ermentrout, G. & Cowan, J. 1979 Temporal oscillations in neural nets. *J. Math. Biology*, **7**, 265–280.

Féger, J., Robledo, P., & Renwart, N. 1991 The subthalamic nucleus: new data, new questions. In G. Bernardi, M. Carpenter, G. Chiara, M. Morelli, & P. Stanzione, editors, *The Basal Ganglia III*, pages 99–108. Plenum Press, New York.

Fujimoto, K. & Kita, H. 1993 Response characteristics of subthalamic neurons to the stimulation of the sensorimotor cortex in rat. *Brain Res.*, **609**, 185–192.

Gillies, A. & Willshaw, D. 1998 A massively connected subthalamic nucleus leads to the generation of widespread pulses. *Proc. R. Soc. Lond.* **B**, **265**, 2101–2109.

Houk, J. & Wise, S. 1995 Distributed modular architectures linking basal ganglia, cerebellum, and cerebral cortex: their role in planning and controlling action. *Cerebral Cortex*, **2**, 95–110.

Iwahori, N. 1978 A golgi study on the subthalamic nucleus of the cat. *J. Comp. Neurol.*, **182**, 383–398.

Joel, D. & Weiner, I. 1997 The connections of the primate subthalamic nucleus: indirect pathways and the open–interconnected scheme of basal ganglia–thalamocortical circuitry. *Brain Res. Reviews*, **23**, 62–78.

Kita, H. 1992 Responses of globus pallidus neurons to cortical stimulation: intracellular study in the rat. *Brain Res.*, **589**, 84–90.

Kita, H. & Kitai, S. 1991 Intracellular study of rat globus pallidus neurons: membrane properties and response to neostriatal, subthalamic, and nigral stimulation. *Brain Res.*, **564**, 296–305.

Kita, H. & Kitai, S. 1994 The morphology of globus pallidus projection neurons in the rat: an intracellular staining study. *Brain Res.*, **636**, 308–319.

Kita, H., Chang, H., & Kitai, S. 1983a The morphology of intracellularly labeled rat subthalamic neurons: a light microscope analysis. *J. Comp. Neurol.*, **215**, 245–257.

Kita, H., Chang, H., & Kitai, S. 1983b Pallidal inputs to the subthalamus: intracellular analysis. *Brain Res.*, **264**, 255–265.

Levy, R., Hutchison, W., Lozano, A., & Dostrovsky, J. 2000 High-frequency synchronization of neuronal activity in the subthalamic nucleus of Parkinsonian patients with limb tremor. *J. Neuroscience*, **20**, 7766–7775.

Magariños-Ascone, C., Figueiras-Mendez, R., Riva-Meana, C., & Córdoba-Fernández, A. 2000 Subthalamic neuron activity related to tremor and movement in Parkinson's disease. *European Journal of Neuroscience*, **12**, 2597–2607.

Nakanishi, H., Kita, H., & Kitai, S. 1987 Electrical membrane properties of rat subthalamic neurons in an in vitro slice preparation. *Brain Res.*, **437**, 35–44.

Nambu, A. & Llinás, R. 1994 Electrophysiology of globus pallidus neurons in vitro. *J. Neurophysiology*, **72**, 1127–1139.

Nini, A., Feingold, A., Slovin, H., & Bergman, H. 1995 Neurons in the globus pallidus do not show correlated activity in the normal monkey, but phase–locked oscillations appear in the MPTP model of Parkinsonism. *J. Neurophysiology*, **74**, 1800–1805.

Plenz, D. & Kitai, S. 1999 A basal ganglia pacemaker formed by the subthalamic nucleus and external globus pallidus. *Nature*, **400**, 677–682.

Plenz, D., Herrera-Marschitz, M., & Kitai, S. 1998 Morphological organization of the globus pallidus–subthalamic nucleus system studied in organotypic cultures. *J. Comp. Neurol.*, **397**, 437–457.

Redgrave, P., Prescott, T., & Gurney, K. 1999 The basal ganglia: a vertebrate solution to the selection problem? *Neuroscience*, **89**, 1009–1023.

Shamma, S. 1989 Spatial and temporal processing in central auditory networks. In C. Koch & I. Segev, editors, *Methods in Neuronal Modeling*, pages 247–289. MIT Press, Massachusetts.

Shink, E., Bevan, M., Bolam, J., & Smith, Y. 1996 The subthalamic nucleus and the external pallidum: two tightly interconnected structures that control the output of the basal ganglia in the monkey. *Neuroscience*, **73**, 335–357.

Smith, Y. & Bolam, J. 1989 Neurons of the substantia nigra reticulata receive a dense gaba-containing input from the globus pallidus in rat. *Brain Res.*, **493**, 160–167.

Smith, Y., Wichmann, T., & DeLong, M. 1994 The external pallidum and the subthalamic nucleus send convergent synaptic inputs onto single neurons in the internal pallidal segment in monkey: Anatomical organization and functional significance. In G. Percheron, J. McKenzie, & J. Féger, editors, *The Basal Ganglia IV*, pages 51–62. Plenum Press, New York.

Smith, Y., Bevan, M., Shink, E., & Bolam, J. 1998 Microcircuitry of the direct and indirect pathways of the basal ganglia. *Neuroscience*, **86**, 353–387.

Suri, R. & Schultz, W. 1998 Learning of sequential movements by neural network model with dopamine–like reinforcement signal. *Exp. Brain Res.*, **121**, 350–354.

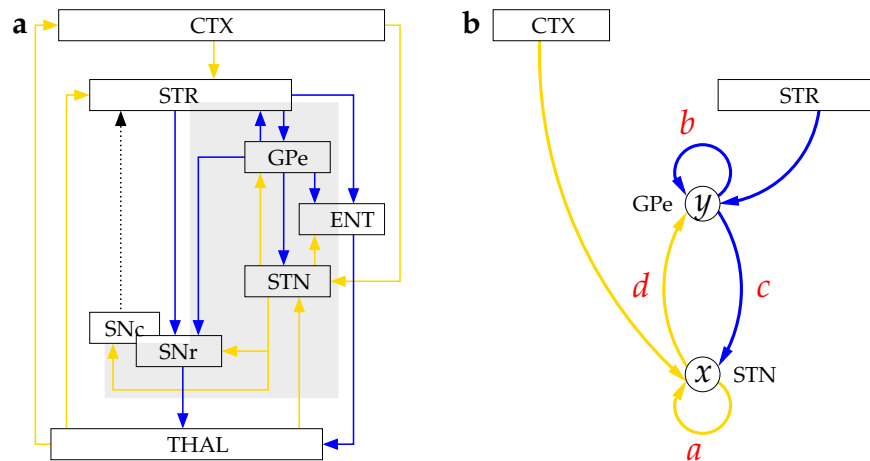Wichmann, T. & DeLong, M. 1999 Oscillations in the basal ganglia. *Nature*, **400**, 621–622.

Figure 1: **a**, The major pathways through the basal ganglia. The shaded area denotes the indirect pathway from striatum to substantia nigra and entopeduncular nucleus. CTX, cortex; STR, striatum; STN, subthalamic nucleus; GP, globus pallidus; THAL, thalamus; SNr, substantia nigra pars reticulata; SNc, substantia nigra pars compacta; ENT, entopeduncular nucleus. Blue pathways indicate inhibitory connections, yellow pathways indicate excitatory. The dotted line represents a dopaminergic projection. **b**, Schematic diagram of the interactions between and within STN and GP. x, y indicate the potentials in mV of STN and GP neurons respectively. a,b,c,d are the coupling parameters for the interactions within and between nuclei, converting firing rates into potentials in mV. For details of the equations used see Box 1.
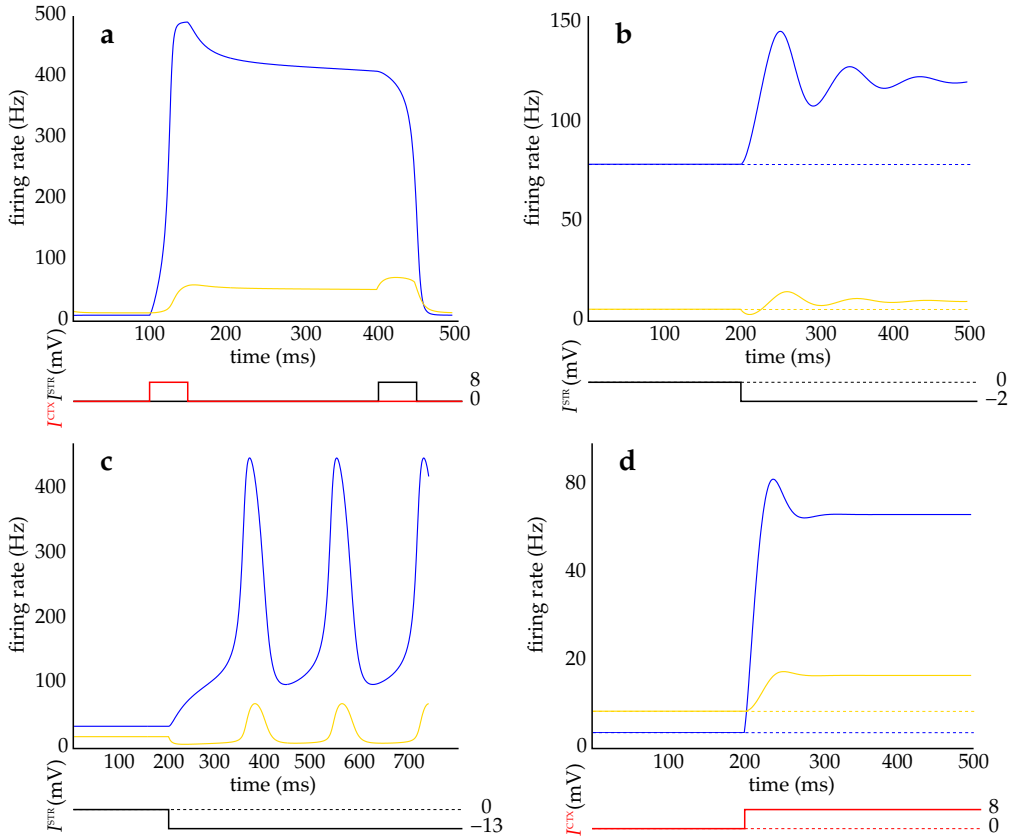
Figure 2: Example simulations of the STN–GP system. In all graphs blue and yellow lines represent firing rate of the STN and GP respectively. **a**, Bistable Behaviour. Brief stimulation of the STN at $t = 100$ ms pushes the system from a low state to a sustained high state. *Excitation* of the GP at $t = 400$ ms returns the system to the low state (such excitation may arise from GP afferents or from internal cell properties - see Gillies & Willshaw, 1998). **b**, Increased inhibition of the GP at $t = 200$ ms increases the mean activities of both the STN and GP. **c**, Oscillations. An increase in the inhibition (I^{STR}) at $t = 200$ ms results in system oscillation. **d**, increased excitation to the STN increases the mean activities of both the STN and GP. Parameters in all simulations: $\sigma_{\max} = 500$ Hz, $\kappa = 0.3$ mV^{-1}, $x_{\text{th}} = 15$ mV, $\xi_{\max} = 100$ Hz, $\eta = 0.2$ mV^{-1}, $y_{\text{th}} = 10$ mV, $\tau^{\text{STN}} = 6$ ms, $\tau^{\text{GPe}} = 14$ ms, $a = 50\,\mu$VHz^{-1}, $b = 100\,\mu$VHz^{-1}, $d = 80\,\mu$VHz^{-1}, $c = 120\,\mu$VHz^{-1}. Variations are: **a**, $b = 140\,\mu$VHz^{-1}, $d = 40\,\mu$VHz^{-1}, $c = 10\,\mu$VHz^{-1}. **b**, $I^{\text{CTX}} = 8$ mV. **c**, $I^{\text{CTX}} = 9$ mV. $a = 54\,\mu$VHz^{-1}. **d**, $I^{\text{STR}} = 0$ mV.
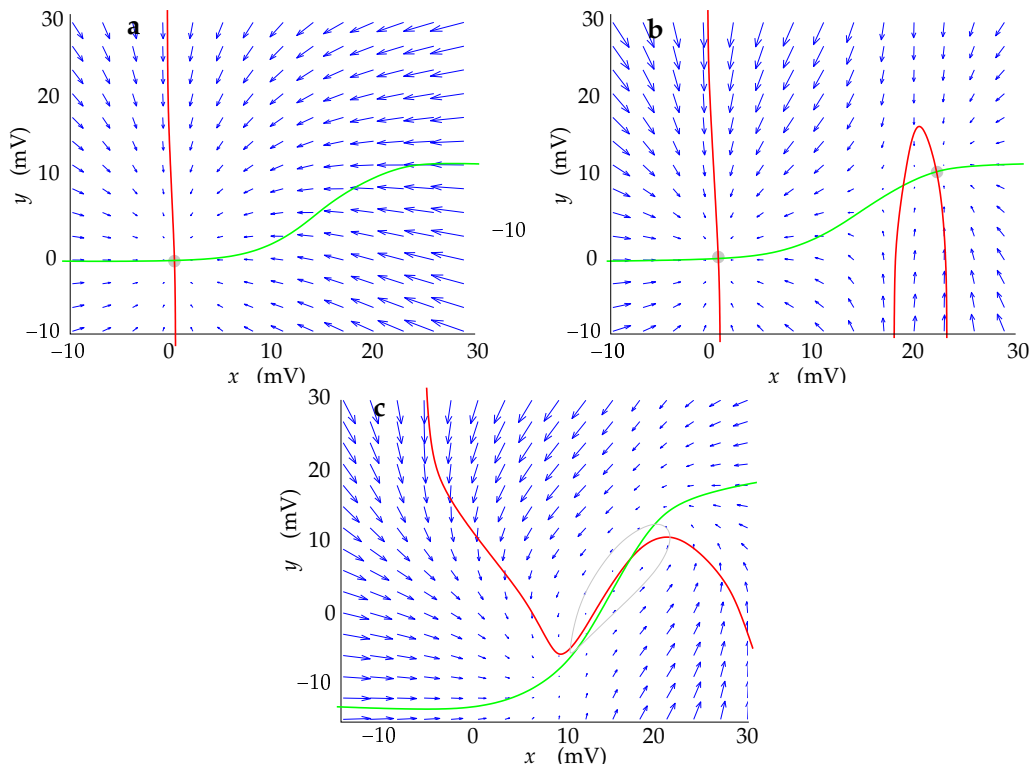
18

Figure 3: Phase plots of the nullclines for (x, y) showing the lines of $dx/dt = 0$ (red) and $dy/dy = 0$ (green) in the (x, y) plane. **a**, under parameter conditions with no connectivity within the STN, i.e., $a = 0$ (all other parameters are the same as the bistable condition given in Fig. 2a) . **b**, under bistable parameter conditions. **c**, under parameter conditions leading to oscillations (see Fig. 2c). Stable points and limit cycles are indicated in gray.
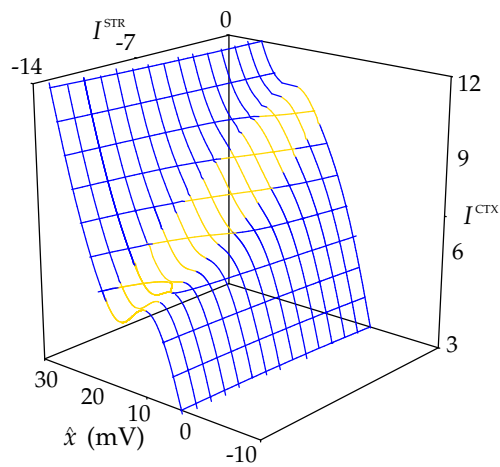
Figure 4: Diagram illustrating the influence of cortical (I^{CTX}) and striatal (I^{STR}) inputs on oscillatory behaviour. The value of the fixed point $\hat{x}$ is plotted against I^{CTX} and I^{STR}. Blue indicates regions of stable fixed point solutions and yellow indicates regions of unstable fixed points solutions associated with oscillations, i.e. every point in the yellow region is a solution where the system is in stable oscillation. As inhibitory input from the striatum to the GP is increased, less excitatory cortical input to the STN is required to generate oscillations. Cortical input is plotted unconventionally on the z-axis and STN activity ($\hat{x}$) on the x-axis to highlight this relationship.